Available online at www.sciencedirect.com
SCIENCE DIRECT®
Clinical Biomechanics 20 (2005) 455–464
CLINICAL BIOMECHANICS
www.elsevier.com/locate/clinbiomech

The prediction of lumbar spine geometry: method development and validation

Naira Campbell-Kyureghyan [a], Michael Jorgensen [b], Deborah Burr [c], William Marras [a,*]

[a] Biodynamics Laboratory, IWSE Department, The Ohio State University, 1971 Neil Ave, Columbus, OH 43210, USA
[b] IME Department, Wichita State University, Wichita, KS 67260, USA
[c] School of Public Health, The Ohio State University, Columbus, OH 43210, USA

Received 20 January 2004; accepted 19 January 2005

Abstract

Objectives. To develop and validate a new method of predicting the neutral lumbar spine curve from external (non-invasive electrogoniometer) measurements.

Background. Non-invasive techniques for lumbar spine geometry prediction suffer from a lack of a complete geometry description, problems with applicability to field conditions, or both.

Methods. The study consisted of three steps. First, utilizing lateral imaging (MRI and X-ray pictures) of the lumbosacral junction, the torso geometry was described using measures of lumbar lordosis via the Cobb method. Second, the relationship between imaging based measurement of lumbar spinal curvature and externally measured torso flexion angle in the sagittal plane using a goniometer was determined. Finally, method validation was performed with an independent set of nine subjects. The predicted lumbar spine curve was determined and the prediction errors were analyzed against the measured curves from digitized lateral X-ray images of the lumbosacral junction.

Results. The shape of the lumbar curve was described as function of three externally measured parameters. The lumbar spine Cobb angle, segmental centroid positions (S_1-T_{12}), and segmental orientations were predicted from the external lumbar motion monitor measurements, with average precisions of 5.8°, 4.4 mm, and 3.9°, respectively.

Conclusions. The position and orientation of each segment (vertebrae and disc), along with the lumbar spine lordosis, can be predicted in the neutral posture using data from back angular measurements.

Relevance

The consideration of the spine as a curve is necessary to accurately quantify and describe the forces acting along the (lumbar) vertebral column for any given loading. The method could be a very useful prediction tool for industrial and laboratory experiments, as well as analytical models.

Keywords: Lumbar lordosis; Lumbar motion monitor; Vertebral position; Geometric model; Model validation

1. Introduction

There are believed to be many different causes of work-related low back disorder (LBD). One path to an understanding of the etiology of low back pain is biomechanics. Many researchers have developed biomechanical models of the spine that are intended to predict and quantify the source and effects of spinal forces. The models have proven useful, but the representation of the lumbar spine as a straight line is a limitation of many of existing models. The curvature of the

* Corresponding author.
E-mail address: marras.1@osu.edu (W. Marras).

0268-0033/$ - see front matter © 2005 Elsevier Ltd. All rights reserved.
doi:10.1016/j.clinbiomech.2005.01.006

spine is one of the important characteristics for determining posture and load bearing function, and hence, the distribution of forces in the spine, particularly in changing posture (Aspden, 1989; Jorgensen et al., 2003a,b).

The spine is not a rigid body; rather it is a multi-joint structure with non-linear geometry, and this fact must be considered in biomechanical models of the lumbar spine. Given that the lumbar spine shape can vary broadly between people, the load distribution and resulting motion will also differ between individuals. Therefore, a subject-specific approach to determining the lumbar spine geometry is preferred for model application.

Accurate prediction of the geometry of the lumbar spine is also important in assessing low-back stress during various work activities. In the past, imaging techniques, such as radiography, computer tomography (CT), or magnetic resonance imaging (MRI) has been the most widely used technique for obtaining lumbar spine geometry. However, these methods are costly, inappropriate for field measurements or industrial settings, and require licensed technicians for implementation. They are also not recommended for all subjects, e.g. pregnant women or for prolonged, repeated exposure. Therefore, it would be advantageous to develop a non-invasive method for evaluating the lumbar spine geometry, based upon easily obtained measures of trunk posture.

Several non-invasive methods for spine geometry evaluation have been described in the literature. These include: skin markers (Stokes et al., 1987; Bryant et al., 1989; Sicard and Gagnon, 1993; Lee et al., 1995; Chiou et al., 1995, 1996), external marker photo- or videography (Davis et al., 1965; Kumar, 1974; Nordin et al., 1986; Chen and Lee, 1997), electromagnetic devices (Nelson et al., 1995; McGill and Kippers, 1994), flexible tape measurement (Anderson and Sweetman, 1975; Burton, 1986; Stokes et al., 1987), ultrasonic digitizer (Letts et al., 1988), and others. These approaches found only limited application in biomechanical models and elsewhere since they either provided little information about the actual spine geometry (due to differences in skin and spinal profiles), were difficult to apply in the field, or both.

In comparison to imaged-based methods (MRI, X-ray, etc.), the benefits of non-invasive methods of spine geometry prediction are clear, provided accurate predictions can be obtained. Therefore, the method of prediction should be based on a tool or device that is applicable to real working environments as well as laboratory settings. In addition, the method should be inexpensive and allow for quick measurements that will permit screenings of large groups. An electrogoniometer is well suited for this task, and this study utilized the Lumbar Motion Monitor (LMM).

The main goal of this study was to develop and evaluate the performance of a non-invasive lumbar spine geometry assessment method to predict the position and orientation of the lumbar vertebral bodies in the upright neutral posture, using an electrogoniometer (LMM). The LMM is essentially an exoskeleton of the spine developed and validated at the OSU Biodynamics Laboratory (Marras et al., 1992) and has been extensively used for data collection protocols for the past decade (Marras et al., 1993, 1994, 1995, 1999). This method brings a new subject-specific perspective to biomechanical modeling of the spine and allows more prudent, detailed and level-specific calculations of stresses on the spine.

2. Methods

2.1. Subjects

A total of 39 subjects with no history of back pain participated in this study on a voluntary basis. Spine images in the sagittal plane were obtained from 24 subjects using MRI (Jorgensen, 2001), and from 15 subjects using radiography. Torso posture using the LMM was also measured on 24 of the 39 subjects, where the data for 14 subjects (8 males and 6 females) were used for model development, and the data from 10 subjects (7 males and 3 females) was used for model validation.

The mean age of the subjects used for model development was 24.4 years (SD 3.9) and the mean spine length (SD) between the S_1 and C_1 levels for males was 60.5 (3.8) cm and for females was 52.6 cm (2.8 cm). The mean and standard deviation of height and weight were 172.4 cm (4.7 cm) and 66.0 kg (6.7 kg) respectively.

The age of the subjects in the validation study ranged from 23 to 32 years with a mean of 26.4 years. The mean and standard deviation of height and weight were 170.7 cm (7.1 cm) and 69.3 kg (16.1 kg), respectively. One subject was later excluded from the data analysis due to spine abnormality (kyphosis). Therefore, the final model performance was tested on a set of nine subjects who had not been used for the model development.

The Human Subjects Committee at the Ohio State University approved the protocol for human subjects in both studies.

2.2. Data collection

The data collection for this study consisted of two steps.

Imaging: Sagittal plane T1 weighted MR imaging of the lumbar spine was performed using a 0.3 T Hitachi Aisis Open MRI at a local hospital, with TR = 400 and TE = 10. The subjects lied within a large size body coil, on top of a wooden peg board with markers and landmark location points drawn on the board to position the subject in each torso posture of neutral, 15, 30 and 45° flexion. Thus, the torso was aligned along the

line between S_1 and C_7 to represent the torso angle, consistent with other studies that measured external torso flexion (Mitnitski et al., 1998). To minimize coronal sagging of the lumbar spine in the lateral recumbent posture, position padding was used in several locations (Jorgensen, 2001). Sample scans at the 0 and 30° flexion angles are shown in Fig. 1.

Radiograph images were taken by a professional X-ray technician using standard, proven safety precautions. One lateral lumbar radiograph was taken for 0 and 30° of torso flexion for each of the 15 subjects using a Eureka Rad-14 X-ray tube (Eureka X-Ray Tube, Inc., 3250 N. Kilpatrick Ave. Chicago, USA). The subjects were standing in an upright position with the right side of the body facing the film. The radiation dose ranged from 60 to 280 ms (120 on average) and 75 KVP. The distance between the 14×17 radiographic films and the tube was 100 cm. Special radiographic markers, 10 cm apart, were placed on the subjects back to allow for scaling of the X-rays to account for the magnification factor.

Goniometric measures: External non-invasive measurements were collected using the LMM, which measures the angular position between the pelvis and the top of the twelfth thoracic vertebra. In order to provide meaningful results, the LMM size (four available) must be selected to match the pelvis-T_{12} measurement of each subject. For this study, LMM measurements were collected at trunk angles of 0 and 30° with the subjects secured at the shoulders in a torso angle reference frame. Additionally, to eliminate the contribution of pelvic rotation on lumbar curvature, orientation, and LMM measurements, the subjects pelvis was stabilized in a pelvic support structure during LMM measurements.

2.3. Model development

Using a computerized digitizing table and custom software, the coordinates of the vertebral body corners (superior and inferior, anterior and posterior) for each level from S_1 to T_{12} were obtained. The anterior and posterior curves were each outlined by the series of 13 digitized points for which the y- and z–coordinates were determined. The centroidal coordinates for all vertebral surfaces (superior and inferior) were calculated by averaging the anterior and posterior coordinates of each vertebral surface. Subsequently, all data were normalized relative to the superior surface centroidal position of S_1 as shown in Fig. 2.

A description of the lumbar spine geometry was constructed based on four parameters: the length of the lumbar spine, the position of T_{12} relative to S_1, the angle of inclination of either T_{12} or S_1, and the difference in angle between them. Since it is impossible to directly measure the actual curved length of the lumbar spine using non-invasive methods, the straight-line length between the superior endplates of S_1 and T_{12} was used to quantify the lumbar spine length, L_0 (Fig. 3). Assuming

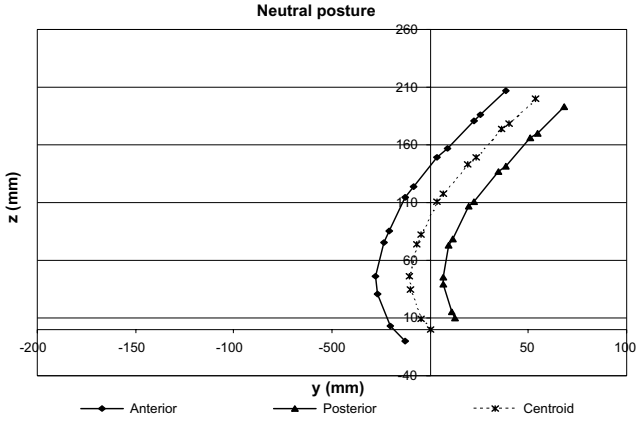

Fig. 2. Graphical representation of the sagittal plane lumbar spine curve (S_1-T_{12}) for one subject. The anterior and posterior curves were obtained from the digitized MRI and the centroidal curve is the average of the anterior and posterior values.

Fig. 1. Sagittal MRI scan of torso in (a) neutral position and (b) 30° forward flexion.

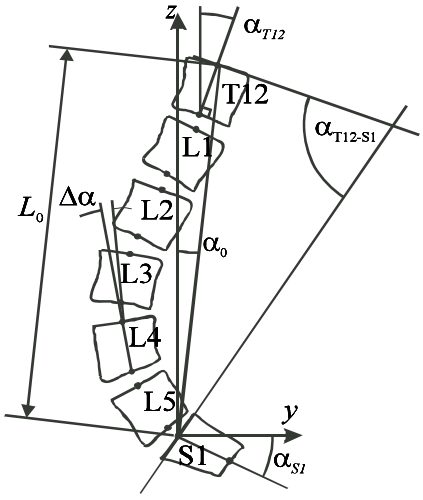

Fig. 3. Sagittal plane view of the lumbar spine in the upright position showing the estimating parameters. The straight-line length between the superior surfaces of S_1 and T_{12} is L_0 and α_0 is the straight-line angle relative to vertical. The Cobb angle, α_{T12-S1}, is defined as the angle between the superior surfaces of S_1 and T_{12}. The angles of S_1 and T_{12} with respect to the horizontal and vertical, respectively, are α_{S1} and α_{T12} while the change in angle between any two segments is denoted as $\Delta\alpha$.

the distance (straight line) between S_1 and T_{12} is known, the position of T_{12} relative to S_1 can be determined if the orientation of the straight line is also known.

Knowing the position of the top and bottom of the lumbar spine, the curve can be estimated if the angle of either the T_{12} or S_1, and the difference in angle between them are known. There are a variety of methods for measuring lumbar lordosis in the literature: TRALL, Cobb, centroid and Harrison posterior tangent methods (Troyanovich et al., 1997; Chen, 1999; Harrison et al., 2001). Selection of the level at which lordosis is measured can also be a significant factor, with the Cobb method between the T_{12} and S_1 levels showing the most consistency (Polly et al., 1996). Based on a literature review and the physical properties of the LMM (top at T_{12}), the $T_{12}-S_1$ Cobb angle was chosen as the lordosis measure for this study and is defined as the difference between the angles describing the superior surfaces of S_1 and T_{12}.

Once the data was collected and digitized, the required geometric parameters were calculated. The angle of the straight line between the superior surface centroids of S_1 and T_{12}, the individual spinal segment angles (vertebrae and disc) with the vertical axis, and the Cobb angle were calculated using Eqs. (1)–(3)

$$\alpha_0 = \operatorname{atan}\left(\frac{y^s_{T12} - y^s_{S1}}{z^s_{T12} - z^s_{S1}}\right) \tag{1}$$

$$\alpha_j = \operatorname{atan}\left(\frac{y^s_j - y^i_j}{z^s_j - z^i_j}\right) \tag{2}$$

$$\alpha_{T12-S1} = \alpha_{T12} - \alpha_{S1} \tag{3}$$

where α_0 is the neutral straight line angle between the superior surface centroids of the S_1 and T_{12} segments, α_j is the neutral angle of segment j with the vertical axis, α_{T12-S1} is the lumbar curvature angle between the superior surfaces of T_{12} and S_1 vertebrae using the Cobb method, y is the horizontal coordinate of the segment surface centroid, z is the vertical coordinate of the segment surface centroid, and the superscripts s and i indicate the superior and inferior surfaces respectively (Fig. 3).

Additionally, the height of each spinal segment, defined as the distance between the superior and inferior surface centroids, was calculated from the digitized data of all 39 subjects. The mean (SD) of the segment heights and angles for all 39 subjects is shown in Table 1. The disc and vertebral heights were within the range of data from previous studies (Tibrewal and Pearcy, 1985; Gilad and Nissan, 1986.

2.4. Geometry prediction

The lumbar spine geometry model developed in this study predicts the centroidal coordinates and orientation angles of the spinal segment ends for the torso in a neutral posture. The entire procedure is depicted in

Table 1
Mean (SD) intervertebral disc and vertebral body heights and orientation angles with respect to vertical for the 39 subjects for whom MRI or radiographic images were collected

Intervertebral disc			Vertebra		
Level	Height (mm)	Angle (°)	Level	Height (mm)	Angle (°)
T12/L1	7.3 (1.2)	14.24 (8.5)	T12	28.9 (3.2)	14.18 (8.8)
L1/L2	8.4 (1.3)	13.2 (8.0)	L1	30.2 (3.3)	13.37 (8.4)
L2/L3	9.3 (1.3)	8.3 (6.6)	L2	31.3 (3.4)	10.92 (7.2)
L3/L4	10.1 (1.3)	0.32 (6.7)	L3	31.0 (3.4)	4.58 (6.7)
L4/L5	10.5 (1.5)	−11.65 (6.8)	L4	31.4(3.2)	−5.12 (6.8)
L5/S1	9.4 (1.44)	−30.3 (7.6)	L5	29.1 (3.1)	−20.96 (7.0)
			S1	–	−35.19 (7.9)

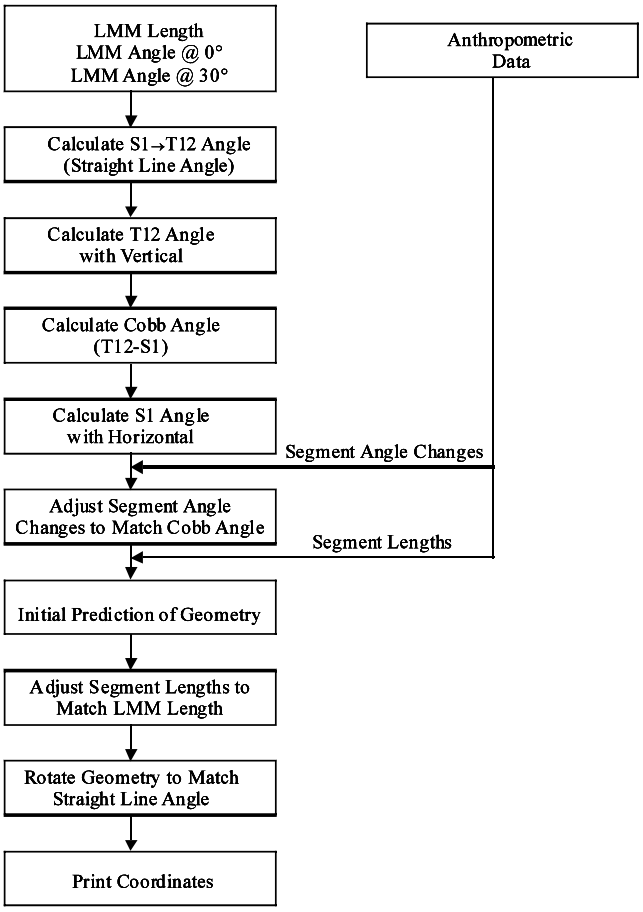

Fig. 4. Flow chart of the model computational procedure.

Fig. 4 and described in this section. Input to the prediction model consists of the estimated value of the lumbar spine length (L_0) and the goniometric measured angles at 0 and 30° trunk angles. Average data (39 subjects) for the vertebrae and disc heights and the angles between the spinal segments ($\Delta\alpha$) are embedded in the prediction program. Based on the input data and the prediction equations described below, the straight-line angle between S_1 and T_{12} (α_0) is first predicted. Predictions of the T_{12} angle with respect to the vertical (α_{T12}) and the Cobb angle (α_{T12-S1}) are then performed and the angle of S_1 (α_{S1}) is calculated based on the predicted angles. The remainder of the procedure reconciles the average data to the data predicted from the goniometric readings.

The sum of the measured inter-segment angle changes gives an "average" value of the Cobb angle. The individual measured inter-segment angle changes are uniformly scaled so that the average Cobb angle matches the predicted Cobb angle. The revised segment angles are used in conjunction with the average segment heights to obtain an initial prediction of the lumbar spine geometry (x- and y-coordinates of the segment end centroids). The straight-line length (L_0) of the predicted geometry will not match the actual straight-line length as determined by the LMM length (see Fig. 3). Therefore, the segment lengths are uniformly scaled so that the final straight-line length matches the LMM length.

The entire lumbar spine geometry is rotated to align with the predicted straight-line angle. Finally, the centroidal coordinates of each segment surface and the segment orientations can be determined.

2.5. Error analysis

The model output consists of the centroidal position of the superior and inferior surface of each vertebrae (and hence of the discs) from the top of S_1 to the top of T_{12}. Since the position of the superior surface of S_1 is "fixed" at (0,0) for both the measured and predicted coordinates, there are no error values for S_1. In order to validate the prediction, the model results were compared to the X-ray images. Error analysis was performed for several different measures. First, the overall performance of the three model formation parameters described above (α_0, α_{T12}, and Cobb angle) was evaluated using the absolute error and difference between the measured and predicted values.

Second, the model precision was evaluated using the absolute linear position error for the top centroids of each of the 12 segments (six discs and six vertebrae), calculated as the distance between the predicted and measured positions as

$$D_j = \sqrt{(y_j - y'_j)^2 + (z_j - z'_j)^2} \quad j = 1, \ldots, 12 \tag{4}$$

where:

D is the absolute linear distance error between measured and predicted surface centroid;
j is the sequential counter for the top of each segment ($S_1 - T_{12}$, including discs);
y and y' are the measured and predicted horizontal coordinates;
z and $z'$are the measured and predicted vertical coordinates.

Finally, the orientation error of each segment was determined as the difference between the measured and predicted values and the absolute angular error of each segment and was calculated as

$$A_j = |\alpha_j - \alpha'_j| \quad j = 1, \ldots, 12 \tag{5}$$

where:

A_j is the absolute orientation error;
α_j and α'_j are the measured and predicted angle of each segment with vertical.

The overall model performance was determined by taking the average for all nine subjects for each error measures.

3. Results

3.1. Model parameters

Three major parameters as described above must be determined for constructing the lumbar curvature using the LMM. The first parameter is the S_1–T_{12} straight-line angle (α_0), which is impossible to measure directly and therefore estimated from external measurements. Since there is a difference between the actual internal straight-line and an externally measured one, the relationship between the two was established by regressing the externally measured torso angle on the image-based data. The resulting linear relationship ($R^2 = 0.79$) was

$$\alpha_0 = 1.6583 \times lmm_0 + 0.3786 \quad (6)$$

where α_0 is the initial straight line angle between the S_1 and T_{12} segments and lmm_0 is the measured LMM angle at 0° trunk angle (neutral).

The second required parameter is the angle of T_{12} with the vertical (α_{T12}). Since the top of the LMM is positioned at the twelfth thoracic vertebrae, and the orientation of T_{12} in the neutral posture should be related to the S_1–T_{12} line orientation, logically there should also be a relationship between the T_{12} angle and the LMM angle. This relationship was identified from a linear regression ($R^2 = 0.57$) of the LMM neutral posture and the digitized data as

$$\alpha_{T12} = 0.9129 \times lmm_0 - 0.0008 \quad (7)$$

where α_{T12} is the initial angle of T_{12} and lmm_0 is the measured LMM angle at 0° trunk angle (neutral).

The third parameter to be determined is the angle of S_1 with the horizontal (α_{S1}). Knowledge of the Cobb angle as well as the T_{12} angle determined above, will allow the calculation of the S_1 angle. Examination of the relationship between the digitized data and LMM measurements show that a quadratic relationship allows for reasonable predictions of the Cobb angle (α_{T12-S1}) ($R^2 = 0.78$). The resulting relationship is

$$\alpha_{T12-S1} = -0.1652 \times (lmm_{30})^2 + 8.6107 \times lmm_{30} - 156.83 \quad (8)$$

where α_{T12-S1} is the Cobb angle between the T_{12} and S_1 segments and lmm_{30} is the difference between the LMM angles at 30 and 0° sagittal trunk flexion.

3.2. Model performance

3.2.1. Model parameters prediction

The accuracy of the equations for the straight-line angle (α_0), Cobb angle, and the T_{12} angle is presented in Table 2. The average difference between the predicted and measured values, the average absolute value of the difference, and the percentage error of the predicted values are also presented. Whether positive or negative, the average difference estimates the bias in the measurement process (over- or underpredicted), and the average absolute difference estimates the error, in either direction. For example, for the straight-line angle, α_0, from the difference we can determine that the prediction is underestimating the true value less than one degree on average. The absolute error shows that the prediction averaged 1.8° distance from the measured value.

Table 2
Mean (SD) and error analysis of the model parameters α_0 (initial straight-line angle with vertical), the Cobb angle defined between the superior surfaces of S_1 and T_{12}, and the T_{12} angle with respect to the vertical for a neutral trunk posture

	α_0 (°)	Cobb angle (°)	T_{12} angle (°)
Measured	−11.1 (4.2)	−60.7 (11.8)	22.7 (7.3)
Predicted	−10.1 (4.7)	−54.8 (8.25)	17.4 (2.6)
Difference	−0.97 (1.97)	−5.8 (8.3)	5.3 (5.8)
Absolute error	1.8 (1.1)	8.8 (4.5)	6.6 (4.0)
Relative error (%)	16.2	14.5	29.1

3.2.2. Model precision

Averages and standard deviations for the absolute position error (D_j) are shown in Fig. 5 for the superior surfaces of the twelve lumbar segments. The position error increases with the height above S_1, with a sudden increase at T_{12}. Since the model origin is fixed at the superior surface of the S_1 vertebra (zero error), it is expected that errors will accumulate as the prediction is generated, thus increasing with height. The average position error for all levels is 4.4 mm with the T_{12} error included and 4.1 mm with it excluded.

The average values and standard deviations of the difference between the predicted and measured segment angles with respect to the vertical and the absolute angular error (A_j) for nine subjects who participated in the validation study are given in Table 3 for each of the twelve lumbar segments. The difference results indicate that there is a slight bias towards overestimating the segment angles, with the bias more evident at the higher levels. The size of the prediction error is given by A_j, indicating greater accuracy for the lower segments, while the scatter in the data is similar at all levels.

The range and standard deviation of the measured segment angles (biological variability) are also shown in Table 3 for the same nine subjects. For example, at the L_3 level, the measured segment angles varied from −10.7 to 14.8° (mean of 4.6) for a total range of 25.4° with a standard deviation of 6.7°. In contrast, the absolute error in the predicted segment angles had a mean of 1.69°. Therefore, in general the likely value of the predicted segment angle lies closer to the subject-specific measured angle than does the average measured angle.

3.2.3. Model validation

Generally, this method performed well in the validation testing. Error analysis showed some variation in

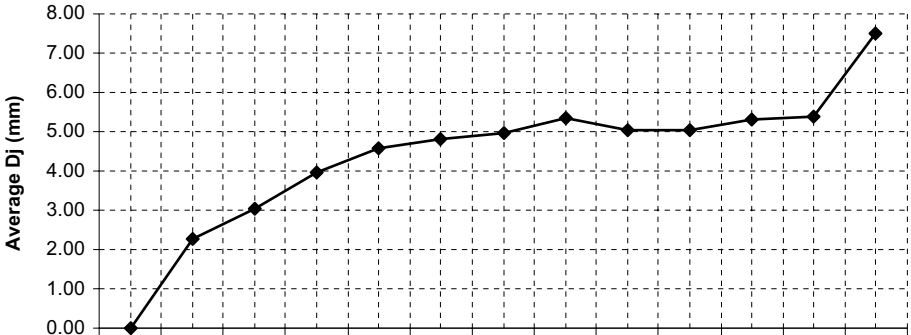

	S1	L5/S1	L5	L4/L5	L4	L3/L4	L3	L2/L3	L2	L1/L2	L1	T12/L1	T12
MEAN	0.00	2.26	3.03	3.96	4.59	4.80	4.98	5.35	5.03	5.03	5.30	5.37	7.52
SD	0.00	0.11	0.10	0.12	0.11	0.13	0.18	0.17	0.25	0.32	0.39	0.45	0.53
% ERROR	0.00	7.02	9.40	12.31	14.39	15.08	15.55	16.55	15.45	15.51	16.56	16.97	24.00

Fig. 5. Mean (graph) and standard deviation of the absolute linear position error for each intervertebral level S_1-T_{12}. The absolute position error, D_j, is defined as distance in mm between the measured and predicted position of the top of each intervertebral segment. The normalized error indicates the percent error relative to a representative physical dimension for each vertebra (S_1, L_5, L_4, L_3, L_2, and L_1) and disc (L_5/S_1, L_4/L_5, L_3/L_4, L_2/L_3, L_1/L_2, and T_{12}/L_1).

Table 3
Arithmetic difference and absolute prediction error (A_j), and range (SD) of measured variability in angle for each intervertebral level from L_5/S_1 to T_{12}

	L5/S1	L5	L4/L5	L4	L3/L4	L3	L2/L3	L2	L1/L2	L1	T12/L1	T12
Diff. (°)	0.31	0.73	−0.03	−0.12	1.20	−0.52	6.07	2.55	6.17	2.74	5.00	6.10
(SD)	(3.9)	(3.9)	(4.5)	(2.5)	(1.8)	(2.0)	(2.4)	(2.3)	(3.4)	(3.1)	(4.3)	(4.8)
A_j (°)	2.91	3.12	3.74	2.27	1.77	1.69	6.07	2.89	6.18	3.86	5.88	6.34
(SD)	(2.4)	(2.3)	(2.3)	(0.8)	(1.3)	(1.1)	(2.5)	(1.8)	(3.5)	(1.2)	(2.8)	(4.5)
Measured variability	35.0	33.2	32.3	31.1	28.7	25.4	24.7	25.4	28.0	30.4	31.8	33.7
Range (°) (SD)	(7.6)	(7.0)	(6.8)	(6.8)	(6.7)	(6.7)	(6.6)	(7.2)	(8.0)	(8.4)	(8.5)	(8.8)

precision of the model parameters. However, the overall shape of the predicted vertebral centroid curve corresponded well with the true shape as measured. The measured and predicted lumbar spine geometries for one subject are shown in Fig. 6.

The model parameter error analysis shows that the T_{12} angle is estimated much less accurately than the other two parameters. Predictions of α_0 and the Cobb angle were more accurate than those of the T_{12} angle (16.2, 14.5, and 29.1% error, respectively). This is an expected trend since the R^2 values of the prediction equations are 0.79 for α_0, 0.78 for the Cobb angle, and 0.57 for the T_{12} angle. In all three cases, the prediction error was less than one standard deviation of the measured data.

The ability to predict the vertebral centroid curve from external goniometric measurements for the lumbar spine had an overall absolute position error of 4.4 mm or 4.1 mm with or without the T_{12} position error included respectively. In order to put the value of this error in perspective, the error as a percentage of the segment width was calculated. The absolute position percentage error ranged from 7 to 24%, varying with the vertebral level. The position error normalized to the corresponding segment width is presented in the

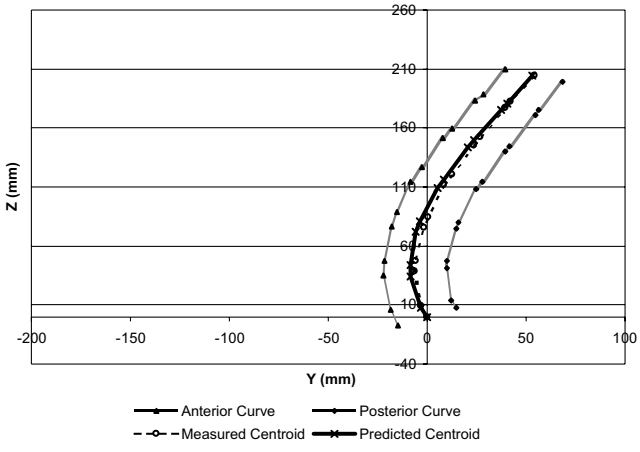

Fig. 6. An illustration of the measured and predicted lateral lumbar spine curves for one subject. The measured anterior and posterior curves were obtained from the digitized radiograph image and the centroidal curve is the average of the anterior and posterior values. The predicted centroidal curve is determined using the model described herein.

bottom line of the table in Fig. 5. The average normalized position error is 14.9% with T_{12} included and 14.0% with T_{12} excluded.

4. Discussion

This paper has introduced a new non-invasive method for lumbar spine geometry prediction based on external goniometric measurements. A relationship has been developed between the LMM angle change during 30° of trunk flexion and the neutral position lordosis of the spine. This relationship is reflected by an R^2 value of 0.78 in the prediction equation. However, a statistical correlation is not, by itself, a sufficient measure.

The concept is relatively straightforward and can be visualized using simplified representations. Take as an example two curves representing lumbar spines with different severity of lordosis, larger (a) and smaller (b) in the neutral position (i) as shown in Fig. 7. If a trunk flexion of α is imposed, the resulting curves (f) are as shown in the figure. During sagittal flexion, the spine with larger curvature can be expected to "unwind" and therefore the distance (L) between two points, the superior surfaces of S_1 and T_{12}, increases as the spine takes on a more nearly linear geometry. In contrast, the flatter spine during rotation α should not be expected to lengthen as much and may even shorten Fig. 7b.

Since the LMM converts changes in length into angular displacement, those measurements can be expected to correlate to the neutral Cobb angle. The physical reasoning is corroborated statistically by the fit of the obtained Cobb angle versus change in LMM angle relationship equation.

Once the basic relationship between LMM angle changes and lumbar curvature was established and explained, the most favorable torso flexion angle for collection needed to be determined. Data collection occurred for 15, 30, and 45° torso flexions for the subjects participating in the MRI study (Jorgensen, 2001).

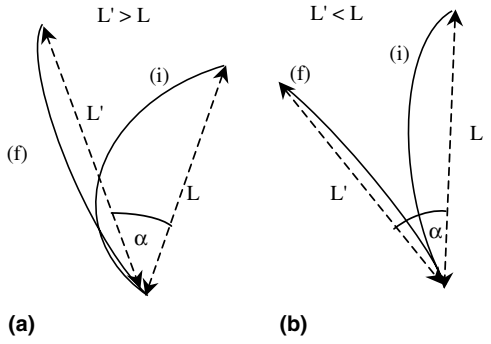

Fig. 7. Illustration of the differences between initial (i) and final (f) positions for straight-line length, L and L' respectively. The effect of (a) large Cobb angle and (b) small Cobb angle in the neutral position are shown.

Subjects with larger degrees of lumbar curvature demonstrated lengthening of the T_{12}–S_1 line for all three torso flexion positions while subjects with flatter spines had inconsistent length changes. Small length changes were observed for 15° of torso flexion while some subjects exhibited kyphosis at 45° flexion. Our findings indicate that the lumbar spine flattens out at around 30° flexion before reversing curvature, as has been seen in other studies (Chen, 1999; Farfan, 1975; Gracovetsky et al., 1977; Kumar, 1974). Therefore, of the three torso flexion angles collected, 30° was determined to best estimate the relationship between the LMM angle change and neutral lordosis. Thus, data were collected at that torso angle for all subjects.

Several other non-invasive methods have been used to predict lumbar spine geometry. These methods reported results for various landmarks such as the centroid of the vertebrae or the anterior and posterior corners. As a result, a direct level-by-level comparison of our results with other geometry prediction methods is difficult. However, it is instructive to look at the range of errors and overall precision of the different models.

Lee et al. (1995) and Chiou et al. (1996) used nonlinear transformations to predict lumbar spine geometry from skin markers, where the average position error for each model was 4.3 mm and 7.2 mm, respectively. Skin profiles using radiopaque markers and a cubic spline transformation were used by Bryant et al. (1989) to generate lumbar spine profiles, with a resulting mean position error of 2.1 mm. Finally, Sicard and Gagnon (1993) used a multi-step nonlinear transformation process to predict lumbar spine geometry from skin markers. With the translation error removed, the resulting mean position error was 3.1 mm.

The overall mean difference between the measured and predicted angles using the current method was 2.5° and the overall absolute error was 3.9° with a standard deviation of 0.9°. As with the position errors, direct level-by-level comparison with previous models is not possible, but there is sufficient data from two studies to determine the overall angular error. Chen and Lee (1997) reported a mean difference in segment angles for the L_1, L_3, and L_5 vertebrae of 4.9°. Sicard and Gagnon (1993) reported a mean absolute error of 4.4° for the neutral posture. Thus the prediction errors from our method are slightly lower than for previously reported methods.

An important part of biomechanical modeling is an understanding of the role geometry plays in the behavior. The distribution and transmission of forces, and muscle orientation and distance from the lumbar spine, are significant parameters in the quantification of stresses on a particular joint of the lower back and are highly dependent on the shape and concavity of the spine (Aspden, 1989; Jorgensen et al., 2003a,b). Analyses of spinal motion and loads typically assume either a linear or an

average geometry. However, no two spines are identical due to the biological variability in material properties, geometry, etc. The lumbar curve is mainly due to differences between anterior and posterior height of the discs, which defines the angle change across the disc. Even if the standing upright torso angles are alike for two subjects, the internal geometry (lordosis) may differ and this will be reflected in the LMM angle changes with flexion. Since this is highly individual, the definition of a ''normal'' spinal curve in general varies considerably from person to person (King, 1995). Therefore, it is clear that subject-specific lumbar spine geometry is required for accurate load and motion prediction, and ultimately, injury prediction and prevention.

Some limitations on the application of the method exist. First, radiographic error can be introduced to the overall validation procedure due to parallax error. In the present study this error was minimized due to the strictly sagital symmetric posture (no twisting) and the high definition of radiographs diminished the digitizing error of the spine segmental landmark positions to approximately 0.5 mm. Second, the model was developed for prediction of the lumbar *lordosis* of a neutral trunk posture and is not appropriate for subjects with kyphosis. Third, this model is limited to predictions of lumbar curvature and position in the sagittal plane and does not address the geometry of the lumbar spine in asymmetric postures. Fourth, the effect of additional axial load on the compression (length) of the soft tissue of the spine, and consequently upon the prediction accuracy, was not investigated. Finally, it has been reported that a variation in stature occurs over the course of a day (Adams et al., 1987; Krag et al., 1990) and with increasing age (e.g., after the 4th or 5th decade [Amonoo-Kuofi, 1992; Gelb et al., 1995]). Since lordosis is due to the differences in height of the anterior and posterior aspects of the disc, these stature variations should indirectly affect posture. The change in posture would be reflected in the LMM angle in the neutral standing upright position, and thus will also affect the predictions of the model parameters, and of the lumbar spine geometry. The current study has not investigated any required changes in the method to account for temporal variations, but further study should provide the required parameters.

5. Conclusions

A new method presented in this paper introduces a non-invasive approach for subject-specific modeling of the geometry of the lumbar spine in a neutral posture. It allows for the accurate representation of the vertebral position and orientation relative to the sacrum using scaled anthropometric data and individual goniometric measurements. The validation study shows that the new, non-invasive prediction method allows for accurate determination of not only the overall lumbar spine curvature, but also of the lumbar spine segmental positions and orientations (S_1 to T_{12}). Since goniometers are widely used for motion studies, the method can be integrated with existing biomechanical models to allow for subject-specific analysis. While the equations used in the prediction method were derived using the LMM, the basic approach should be applicable to any electrogoniometer with proper validation.

Acknowledgments

The authors gratefully acknowledge the assistance of Theresa Palicki, Brenda York and Wendy Albert during X-ray collection.

References

Adams, M.A., Dolan, P., Hutton, W.C., 1987. Diurnal variations in the stresses on the lumbar spine. Spine 12, 130–137.

Amonoo-Kuofi, H.S., 1992. Changes in the lumbosacral angle, sacral inclination and the curvature of the lumbar spine during aging. Acta Anat. 145, 373–377.

Anderson, J.A.D., Sweetman, B.J., 1975. A combined flexi-rule/hydrogoniometer device for measurement of lumbar spine and its sagittal movement. Rheumatol. Rehabil. 14, 173–179.

Aspden, R.M., 1989. The spine as an arch. A new mathematical model. Spine 14, 266–274.

Bryant, J.T., Reid, J.G., Smith, B.L., Stevenson, J.M., 1989. Method for determining vertebral body positions in the sagittal plane using skin markers. Spine 14, 258–265.

Burton, A., 1986. Regional lumbar sagittal mobility: Measurements by flexi-curvs. Clin. Biomech. 1, 20–26.

Chen, Y.L., Lee, Y.H., 1997. A non-invasive protocol for the determination of lumbosacral vertebral angle. Clin. Biomech. 12, 185–189.

Chen, Y.L., 1999. Vertebral centroid measurement of lumbar lordosis compared with the Cobb technique. Spine 24, 1786–1790.

Chiou, W.-K., Chen, W.-J., Lee, M.-Y., Lin, Y.-H., 1995. Predictive model of intersegmental mobility of lumbar spine in the sagittal plane from skin markers. Clin. Biomech. 10, 413–420.

Chiou, W.-K., Lee, Y.-H., Chen, W.-J., Lee, M.-Y., Lin, Y.-H., 1996. A non-invasive protocol for the determination of lumbar spine mobility. Clin. Biomech. 11, 474–480.

Davis, P.R., Troup, J.D.G., Burnard, J.H., 1965. Movements of the thoracic and lumbar spine when lifting: A chrono-cyclophotographic study. J. Anat. 99, 13–26.

Farfan, H.F., 1975. Muscular mechanism of the lumbar spine and the position of power and efficiency. Orthop. Clin. North Am. 6, 135–144.

Gelb, D.E., Lenke, L.G., Bridwell, K.H., Blanke, K., McEnery, K.W., 1995. An analysis of sagittal spinal alignment in 100 asymptomatic middle and older aged volunteers. Spine 20, 1351–1358.

Gilad, I., Nissan, M., 1986. A study of vertebrae and disc geometric relations of the human cervical and lumbar spine. Spine 11, 154–157.

Gracovetsky, S., Farfan, H.F., Lamy, C., 1977. A mathematical model of the lumbar spine using an optimized system to control muscles and ligaments. Orthop. Clin. North Am. 8, 135–153.

Harrison, D.E., Harrison, D.D., Cailliet, R., Janik, T.J., Holland, B., 2001. Radiographic analysis of lumbar lordosis: Centroid, Cobb, TRALL, and Harrison posterior tangent methods. Spine 26, E235–E242.

Jorgensen, M.J., 2001. Quantification and modeling of the lumbar erector spinae as a function of sagittal plane torso flexion. PhD Dissertation, Ohio State University, Columbus, OH.

Jorgensen, M.J., Marras, W.S., Gupta, P., Waters, T.R., 2003a. The effect of torso flexion on the lumbar torso extensor muscle sagittal plane moment arms. The Spine J. 3, 363–369.

Jorgensen, M.J., Marras, W.S., Gupta, P., 2003b. Cross-sectional area of the lumbar back muscles as a function of torso flexion. Clin. Biomech. 18, 280–286.

King, A., 1995. Biomechanics of the spine and pelvis. In: Backaitis, S. (Ed.), Biomechanics of Impact Injuries and Injury Tolerances of the Abdomen, Lumbar Spine, and Pelvis Complex. Society of Automotive Engineers, Warrendale, PA, pp. 55–67.

Krag, M.H., Cohen, M.C., Haugh, L.D., Pope, M.H., 1990. Body height change during upright and recumbent posture. Spine 15, 202–207.

Kumar, S., 1974. A study of spinal motion during lifting. Irish J. Med. Science 143, 86–95.

Lee, Y.-H., Chiou, W.-K., Chen, W.-J., Lee, M.-Y., Lin, Y.-H., 1995. Predictive model of intersegmental mobility of lumbar spine in the sagittal plane from skin markers. Clin. Biomech. 10, 413–420.

Letts, M., Quanbury, A., Gouw, G., Kolsun, W., Letts, E., 1988. Computerized ultrasonic digitization in the measurement of spinal curvature. Spine 13, 1106–1110.

Marras, W., Fathallah, F., Miller, R., Davis, S., Mirka, G., 1992. Accuracy of a three dimensional Lumbar Motion Monitor for recording dynamic trunk motion characteristics. Int. J. Ind. Ergo. 9, 75–87.

Marras, W., Parnianpour, M., Ferguson, S., et al., 1993. Quantification and classification of low back disorders based on trunk motion. Phys. Med. Rehabil. 3, 218–235.

Marras, W., Parnianpour, M., Kim, J., Ferguson, S., Crowell, R., Simon, S., 1994. The effect of task asymmetry, age and gender on dynamic trunk motion characteristics during repetitive trunk flexion and extension in a large normal population. IEEE Trans. Rehab. Eng. 2, 13–146.

Marras, W., Parnianpour, M., Ferguson, S., et al., 1995. The classification of anatomic- and symptom-based low back disorders using motion measure models. Spine 20, 2531–2546.

Marras, W., Ferguson, S., Gupta, P., et al., 1999. The quantification of low back disorders using motion measures: Methodology and validation. Spine 24, 2091–2100.

McGill, S.M., Kippers, V., 1994. Transfer of loads between lumbar tissues during the flexion-relaxation phenomenon. Spine 19, 2190–2196.

Mitnitski, A., Yahia, L., Newman, N., Gracovetsky, S., Feldman, A., 1998. Coordination between the lumbar spine lordosis and trunk angle during weight lifting. Clin. Biomech. 13, 121–127.

Nelson, J.M., Walmsley, R.P., Stevenson, J.M., 1995. Relative lumbar and pelvic motion during loaded spinal flexion/extension. Spine 20, 199–204.

Nordin, M., Greenidge, N., Tauber, C., Ngai, J., 1986. Spinal configuration during lifting. Bull. Hos. Jt. Dis. Orthop. Inst. 46, 31–35.

Polly Jr., D.W., Kilkelly, F.X., McHale, K.A., Asplund, L.M., Mulligan, M., Chang, A.S., 1996. Measurement of lumbar lordosis. Evaluation of intraobserver, interobserver, and technique variability. Spine 21, 1530–1535.

Sicard, C., Gagnon, M., 1993. A geometric model of the lumbar spine in the sagittal plane. Spine 18, 646–658.

Stokes, I.A.F., Bevins, T.M., Lunn, R.A., 1987. Back surface curvature and measurement of lumbar spine motion. Spine 12, 355–361.

Tibrewal, S.B., Pearcy, M.J., 1985. Lumbar intervertebral disc heights in normal subjects and patients with disc herniation. Spine 10, 452–454.

Troyanovich, S.J., Cailliet, R., Janik, T.J., Harrison, D.D., Harrison, D.E., 1997. Radiographic mensuration characteristics of the sagittal lumbar spine from a normal population with a method to synthesize prior studies of lordosis. J. Spinal Disord. 10, 380–386.